International Journal of Engineering

Journal Homepage: www.ije.ir

Experimental Assessment of a Fixed On-Shore Oscillating Water Column Device: Case Study on Oman Sea

H. Yazdi, R. Shafaghat*, R. Alamian

Sea-Based Energy Research Group, Babol Noshirvani University of Technology, Babol, Iran

PAPER INFO

ABSTRACT

Ocean wave is one of the renewable energy resources that these days various devices are used to extract its energy. Oscillating Water Column (OWC) installed on the shore is one of the wave energy absorption systems which has received attention due to its simple structure. Investigation of the pneumatic power is of great importance in such systems as the conversion of wave energy to pneumatic energy is the first step in OWCs' energy conversion cycle. This study aims to assess the power available in a fixed onshore OWC plant according to the wave characteristics of the Oman Sea on the shores of Chabahar. For this purpose, a small-scale model of OWC was tested in the wave tank, and its pneumatic power was evaluated. In these experiments, the effects of various parameters including incident wave height and frequency, the front wall draft and the orifice diameter on the pneumatic power were investigated. The results show that increasing the wave height generally increases the pneumatic power; however, variations of power with the draft depends on the incident wave frequencies. The maximum achieved capture performance and maximum generated pneumatic power of the model are 18% and 0.7 watts, respectively.

doi: 10.5829/ije.2020.33.03c.14

NOMENCLATURE

P	power (Watt)		n	number of tests
w	width of the OWC (m)		f	wave frequency (Hz)
ρ	density (kg/m^3)		D	diameter of the orifice (m)
H	wave height (m)		**Greek Symbols**	
C_g	group velocity (m/s)		η	efficiency
g	gravitational acceleration (m/s^2)		α_l	scale
Fr	Froude number		ω	angular frequency (rad/s)
V	characteristic flow velocity (m/s)		σ	standard deviation
l	characteristic length (m)		λ	wavelength (m)
k	wave number (rad/m)		**Subscripts**	
h	water depth (m)		pnu	Pneumatic
p	pressure inside the chamber (Pa)			

1. INTRODUCTION

Study of renewable energies is of great importance due to the increased demand for energy and also the problems caused by fossil fuels and their limited resources [1-3]. As the ocean has the highest energy density among other types of renewable energies, it has received considerable attention during the recent decade [4]. Various methods have been devised to absorb energy from waves [5-7]. In this regard, the use of wave power plants based on OWC has been considered due to their simple mechanism and structure. An OWC wave energy converter is a hollow structure that is partially filled with water, and the rest is occupied by air [8]. Periodic interaction of waves with

*Corresponding Author Email: rshafaghat@nit.ac.ir (R. Shafaghat)

the device makes the trapped air to compress and decompress above the inner free surface. The generated airflow passes through a one-way turbine which is coupled to a power generator. Because of the low operating cost and simple maintenance of OWCs, they achieved a lot of attention for the extraction of ocean wave energy.

To date, several samples of these devices have been designed and built. These include Pico Project on the island of Pico in Azores, Portugal and LIMPET (Land Installed Marine Power Energy Transmitter) on the island of Islay, Scotland. The Pico plant, having the rated power of 400 kW, was completed in 1999 and the LIMPET, with the rated power of 500 kW, was commissioned at the end of 2000. Another onshore 100 kW OWC plant was built in 2001 in Guangdong Province, China [8]. A large OWC with 1 MW capacity was developed in 2014 by the Oceanlinx Company [9]. The company is looking to build a 5 MW plant in Australia.

Energy conversion cycle of a sample OWC consists of three steps including: (i) wave power is converted to pneumatic power by the water column, (ii) the turbine converts the pneumatic power to mechanical type, and (iii) the mechanical power is converted by the generator into electrical power. Therefore, the total efficiency of this device is affected by the efficiency of turbine, generator and also capture performance of the device which is the ratio of pneumatic power to the incoming wave power. Factors affecting the capture performance include the characteristics of sea at the installation site that are water depth, distance from the coast, wave height and period, etc. as well as the WEC geometry that are dimensions, angles of the front and rear walls, water depth at the edge of the front wall, etc.

There have been many experimental studies in this field. Suroso examined the efficiency of two OWC models (One with reflector and other without reflector) and the effect of wave characteristics on them in various depths [10]. He showed that an increment in the wave period and wave height would increase the pressure. He also showed that the reflector slope variation has a major impact on the pressure inside the chamber so that the efficiency of the model with reflector is approximately twice the efficiency of the model without it. Thomas et al. investigated the hydrodynamic efficiency of an OWC device experimentally [11]. Their experiments focused on the effect of the front wall geometry on OWC efficiency. Their results showed that increasing the front wall submergence reduces the OWC efficiency in short waves. In addition, they demonstrated that the front wall with a rounded edge is more efficient than rectangular geometry. Ram et al. designed an OWC model and tested it in a two-dimensional wave channel [12]. In their model, the air chamber was reduced at the turbine section to obtain the maximum kinetic energy. Experiments were carried out with changes in water depth and wave

frequency. These experiments showed that during the water column rising, the air velocity is always larger compared to water column descending situation. Dizadji and Sajadian designed and optimized an OWC system [13]. Design of the structure is such that the angle of the front and rear walls of the model can be changed. Many experiments were carried out in this study, and the best angles of front and rear walls were obtained. They showed that the air outflow rate in the expansion phase is reduced by 20% as compared with that of the compression phase. In addition, they demonstrated that the air outflow rate increases by raising the wave period and height, and by placing the air outlet tube above the chamber. Sheng et al. investigated the relationship between wave energy conversion efficiency of the OWC device and water column [14]. Their experimental studies were conducted on three different geometries. They found that to generate more energy in a more energetic wave (bigger wave height and wavelength), they needed a larger device. Viviano et al. tested the wave force and reflection on an OWC converter by a large model [15]. Their results demonstrate that an OWC can be combined with a breakwater instead of composite and perforated caissons to reduce the reflection of the waves. Ning et al. tested the hydrodynamic performance of a fixed OWC in a wave flume experimentally [16]. In this study, effects of various parameters including incident wave amplitude, the chamber width, the front wall draught, the orifice scale and the bottom slope on the hydrodynamic efficiency of the OWC device were investigated. They obtained optimal efficiency at an opening ratio of 0.66%. They also demonstrated that the water motion is very dependent on the ratio of wavelength to the OWC width (b/λ).

Looking at the previous studies, it was found that the characteristics of incoming waves and the geometry of OWC is very effective on its optimal performance. Regarding this matter, in the present study, a small model of an OWC is designed and built for evaluation of the power available in a fixed OWC device according to the characteristics of the Oman Sea waves in the Chabahar port. Then, effective parameters on the performance of the model are evaluated using experimental tests in the wave tank. In these tests, influence of the wave height and frequency, the water depth at the lip (draft) and the diameter of air outflow channel on the pneumatic power of this model are examined.

2. THE STUDIED CASE ZONE

2. 1. Characteristics and Location   Wave height is the most important factor in choosing the right location for installation of a wave energy converter. Iran's Renewable Energy Office has provided wave power information for important coastal areas in the north and south of the country (Table 1); the information includes

the power per meter of the coastline, the total length of the coast, and total power of these sites [17-19].

As can be seen in Table 1, Chabahar coast with wave power of 5.8 KW/m and total power of 1539 MW is one of the most suitable areas for absorbing the energy of waves in Iran.

To determine the wave characteristics in the Chabahar region, the results of the project of the Iranian Coastal and Offshore Engineering Directorate named Iranian Seas Wave Modeling (ISWM) were used. This project was carried out jointly by Iran's Oceanographic Studies Center and the Danish Hydraulic Institute (DHI) and includes the characteristics of waves from 1992 to 2002 [20]. According to the official external consultant of the project, the accuracy of results is at least 80%.
The modeling results for the target site, which include the minimum, maximum and average data for different parameters, are presented in Table 2 [20].

2. 2. Wave scaling   Various dimensionless numbers are used for scaling purposes. Scaling based on Froude number is the most common scaling in hydrodynamics of marine structures as gravity plays an important role in the

TABLE 1. Wave power in selected sites in Iran's northern and southern coasts based on the data provided by the Renewable Energy Office [18]

Site name	Power per meter of coastline (kW/m)	Coast length (km)	Total power (MW)
Abadan	2.9	34	101
Abomosa	5.1	5	26
Anzali	3.4	124	423
Astara	0.6	83	50
Babolsar	2.2	155	341
Bandar Abbas	0.9	232	210
Lenge	3.4	359	1222
Bousher	2.2	474	1045
Chabahar	5.8	265	1539
Jask	3.2	289	925
Mahshahr	1.7	223	380
Noushahr	1.1	99	110
Ramsar	1.4	100	141
Siri	5.3	5	27

TABLE 2. The statistical characteristics values of the 10-years modeling in Chabahar port (buoy position) [20]

Parameter	Minimum	Maximum	Average
Significant wave height (m)	0.00	2.45	0.88
Wave period (s)	0.00	10.6	4.68

ocean free surface problems [21]. Froude number is defined as the ratio of inertia force to gravitational force and is expressed as follows:

$$Fr = \frac{V}{\sqrt{gl}} \qquad (1)$$

where V is the characteristic flow velocity, g the gravity and l the characteristic length. Modeling is carried out based on the features of the wave tank of the Babol Noshirvani University of Technology. Table 3 shows the Froude scaling needed for this paper.

According to the waves of the target area, the final aim of this study is to achieve a system with 20 kW net power. Considering 50% loss in turbine and generator, the pneumatic power will be equivalent to 40 kW. As shown in Table 2, the site has waves with heights between zero and 2.5 m and the period between zero and 11 seconds. After a careful review of previous studies, it was found that the laboratory model made at Stellenbosch University, South Africa [22] which has the wave characteristics similar to the waves of Oman Sea, has an average power of 1 watt. To achieve 40 kW pneumatic power, α_l should be equal to 20.7; finally, the scale is considered as 1:22. By selecting the scale of 1:22, the scaled wave height and period of the model should be in the ranges of 0-11 cm and 0-2 seconds, respectively.

3. EXPERIMENTS

3. 1. Energy Capture Performance   As stated in Section 1, the total efficiency of OWC is affected by the efficiency of turbine, generator as well as capture performance of the device, so the expression can be written as follows [9].

$$\eta_{total} = \varepsilon_{capture} \cdot \eta_{turbine} \cdot \eta_{generator} \qquad (2)$$

The generator and turbine efficiency are defined in relations (3) and (4), respectively.

$$\eta_{generator} = \frac{Electrical\ power}{Turbine\ power} \qquad (3)$$

$$\eta_{turbine} = \frac{Turbine\ power}{Pneumatic\ power} \qquad (4)$$

The capture performance is obtained from the ratio of pneumatic power to the incoming wave power as follows.

TABLE 3. Froude scaling for different parameters

Parameter	Scale
Wavelength and wave height	α_l
Wave period	$\alpha_l^{0.5}$
Wave frequency	$\alpha_l^{-0.5}$
Power	$\alpha_l^{3.5}$

$$\varepsilon_{capture} = \frac{P_{pnu}}{P_{wave}.w} \tag{5}$$

where w is the width of the device. For regular waves, P_{wave} is [23]

$$P_{wave} = \frac{1}{8}\rho g H^2 C_g \tag{6}$$

where ρ is the water density, g gravitational acceleration, H wave height, and C_g group velocity expressed as follows.

$$C_g = \frac{1}{2}\frac{\omega}{k}\left(1 + \frac{2kh}{\sinh kh}\right) \tag{7}$$

where h is the water depth, k wave number, and ω angular frequency. k and ω are defined by

$$k = \frac{2\pi}{\lambda} \tag{8}$$

$$\omega^2 = gk\, tanh\, kh \tag{9}$$

Also, the following equation is used to calculate the converter's pneumatic power [13].

$$P_{pnu} = (p + \frac{1}{2}\rho_{air}V^2)V\frac{\pi D^2}{4} \tag{10}$$

p is the pressure inside the chamber, V the velocity of the exhaust air, and D the diameter of the orifice.

3. 2. Experimental Set-up   Experiments were carried out in the wave tank at the Sea-Based Energy Research Group of Babol Noshirvani University of Technology. The wave tank has a length of 11 m and width and height of 3 m [24]. It is equipped with a flap type wave maker. One side of the tank is made of plexiglas windows that allow filming of the waves (Figure 1). The wave tank includes a wave maker system for generating regular waves with desirable length and amplitudes and a wave damper for simulating the seacoast. The wave damper decreases the reversing wave effects on the WEC oscillations. As can be seen in Figure 1, the windows are situated for observation and video capturing.

Figure 2 (a) shows the wave maker system which is controlled by an inverter device located outside of the wave tank. The designed wave maker system has 15 different arm lengths. This enables 15 horizontal displacements of the wave maker plate, so-called paddle, from 6 to 36 cm. This system has a 5kW motor and a 1:10 reduction gearbox; it provides revolutions varying from 10 to 150 rpm for the wave-maker system. The motor attached to the wave maker system is displayed in Figure 2 (b).

Figure 3 shows the damper which is used in the wave tank. This damper can be adjusted in four locations, where its position will be changed according to different depths of still water.

Figure 4 shows the schematic of the OWC model and its dimensions. The slope of the model, 20°, is chosen according to the slope of the damper so that the model is
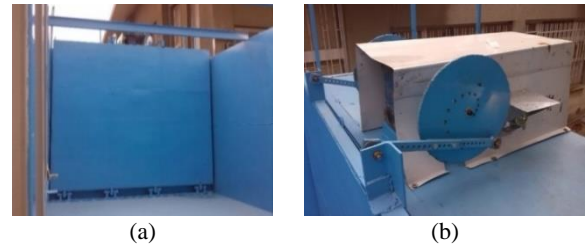

Figure 1. Wave tank and its control room

(a)   (b)

Figure 2. (a) The wave maker system, (b) motor and moving mechanism of the paddle.
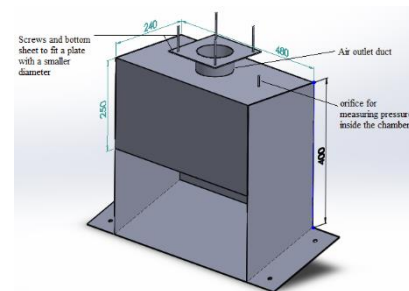

Figure 3. The damper system of the wave tank

Figure 4. Schematic of the OWC model and its dimensions

placed in the vertical position when mounted on the damper.

The model is installed at a distance of 9 meters from the wave maker. Figure 5 provides a schematic layout of the experimental set-up and the positioning of the model and the camera.

To measure the wave characteristics, video analysis is implemented by the Tracker software. Tracker is a Java-based software that allows users to analyze video files. To determine wave characteristics by this software, a buoy has been placed at a distance of 5 m behind the wave-maker (Figure 6). The oscillations of the red spot of the buoy are recorded over time. This software
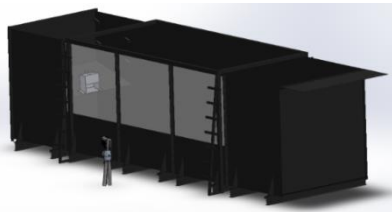
Figure 5. Schematic view of the model in the wave tank

tracks the displacement of this point in time which yields the wave height and period. An example of analysis by this software is shown in Figure 7. The right-hand side curve in this figure shows the vertical displacement of the tip of the buoy over time.

According to Equation (10), for calculation of the pneumatic power, the pressure inside the chamber and the velocity of the outlet air must be measured. For the measurement of the air-chamber pressure, a gauge or differential pressure transducer is required for direct connection to the OWC model [25]. Pressure measurements can be performed at three levels: total pressure, dynamic pressure, and static pressure measurements. For the pressure variations in the air chamber, the static pressure type is used. These measurements were carried out by Trafag pressure transmitter which has a pressure range of 0-0.1 bar (Figure 8).

The Pitot tube was used to measure the outlet air velocity. These measurements were carried out by manometer GM520 (Figure 9). By installing its software, pressure variations with time (Δp-t) was achieved during the test.

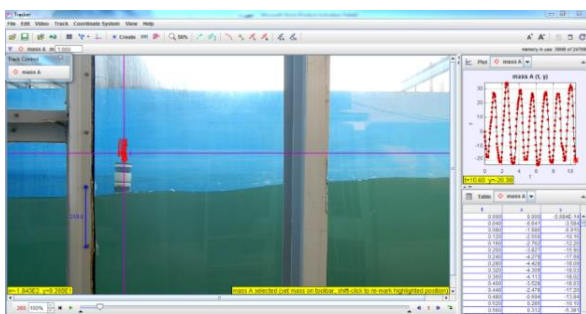**Figure 6.** Buoy in the wave tank to measure the wave characteristics**.**

Figure 7. An example of video analysis by Tracker software

Figure 8. Pressure transmitter Trafag 8473.66.5417

Figure 9. Manometer GM520

To measure the flow rate, the Pitot tube is placed at the air outlet path (Figure 10). Using the Time-pressure diagram recorded by the manometer (Δp-t), the flow velocity is calculated by the following Equation [9]:

$$V = \sqrt{\frac{2\overline{\Delta p}}{\rho_{air}}} \qquad (11)$$

where $\overline{\Delta p}$ is the average pressure derived from the diagram Δp-t. Figure 10 shows how the pressure transducer and manometer are connected to the OWC chamber and the Pitot tube, respectively.

Pressure transducer data was extracted and recorded by using the LabVIEW software. Figure 11 shows an illustration of the software settings.

3. 3. Experimental Procedure   For experimental evaluation of pneumatic devices, such as OWCs, the air turbine can be simulated using an orifice to restrict the airflow and to increase the pressure in the air chamber. Therefore, in the first step, to examine the parameters affecting the performance of an OWC converter, variations of pneumatic power by changing the diameter
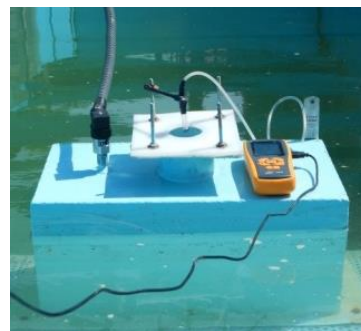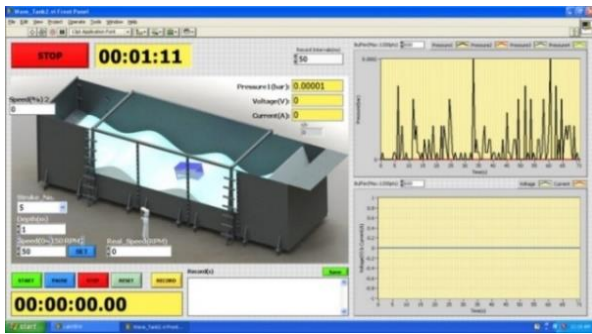

Figure 10. The installed model along with the sensors

Figure 11. An example of the extraction of pressure transducer data in the LabVIEW software

of the outlet orifice was tested. Sheng et al. suggest that the orifice area for optimal power conversion efficiency should be typically between 0.5 to 2.0% of the water column area [23]. Joubert found that an orifice plate hole with an area of 0.7% of the chamber surface area produced the greatest efficiency [26]. Thiruvenkatasamy and Neelamani also reported the ratio of 0.81% for maximum power conversion [27]. Moreover, in the latest study, Ning et al. found that this ratio has a significant influence on the maximum hydrodynamic efficiency of the OWC device [16]. Their results indicate that the optimal efficiency occurs at the opening ratio of 0.66%. In the present study, the effect of air outlet duct on the performance of the converter was investigated in two diameters of 80 and 32 mm. The diameter of 80 mm is the initial size of the air outlet duct, which is selected according to the model of the Stellenbosch University [22], and the diameter of 32 mm corresponds to an orifice with a ratio of 0.7%. These tests were carried out in a 6

cm draft and with a wave height of 8 cm and frequencies of 0.67 Hz and 0.83 Hz.

In the next step, a combination of the parameters of the draft heights and the wave frequencies were tested to evaluate the performance of the model in different drafts. The experiments were carried out in five water drafts, and the effect of wave height and wave frequency on the performance of the device was studied. Table 4 shows the characteristics of the waves as well as the height of the drafts in the model test.

At each frequency, four wave heights have been tested. The classification of the required waves for these experiments is presented in Table 5. To ensure the accuracy of the results, each test was repeated three times.

4. RESULTS AND DISCUSSIONS

4. 1. Extracting the Data   To calculate the pneumatic power of the OWC, first, the pressure variation diagram is extracted. Figure 12 shows an example of the pressure variations in the chamber, recorded by the pressure transducer.

According to Figure 12, it can be seen that the pressure inside the chamber varies according to the wave period, and there is a pressure peak every 1.2 seconds.

TABLE 4. values of test parameters

Wave heights (cm)	Wave frequencies (Hz)	Drafts (cm)
5, 6, 7, 8, 9, 10, 11	0.5, 0.67, 0.83, 1	2, 6, 10, 14, 18

TABLE 5. Classification of waves for tests related to each of the five drafts

f (Hz)	0.5				0.67				0.83				1			
H (cm)	5	6	7	8	6	7	8	9	7	8	9	10	8	9	10	11
Test No.	1	2	3	4	5	6	7	8	9	10	11	12	13	14	15	16
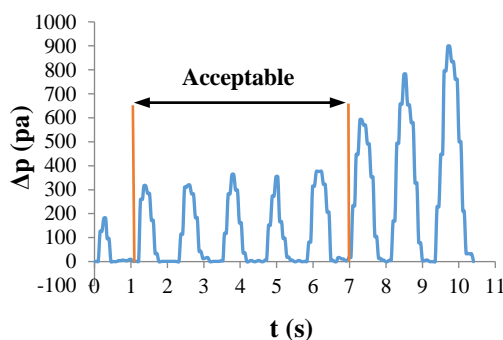
Figure 12. Pressure variations inside the chamber with a wave frequency of 0.83 Hz and a 10 cm height in the 6 cm draft

Because the measuring range of pressure transducer is 0-0.1 bar, hence the compression pressure is only recorded during the test. Therefore, there is only a positive pressure peak at each frequency in the pressure diagram. Since the airflow is periodic, the pressure diagram is oscillatory, as well.

In pressure diagrams, a sudden increase in pressure can be seen after a few seconds; it occurs because of the collision of returning waves from the end of the wave tank with the incoming waves from the wave maker. As shown in Figure 12, the pressure is sharply increased after the seventh second. To calculate the mean pressure, the data before this increment was considered. Furthermore, as can be seen in Figure 12, the data from

the first period of pressure oscillation is also eliminated, because the wave has not reached the OWC yet. This process is carried out for all three replications of the tests; and after determining their mean pressure, the average of these three mean pressures is used for subsequent calculations. In the next step, according to Equation (9), the average velocity is determined, and the pneumatic power of the device is calculated from Equation (6).

The experiments on the effects of the incident waves were carried out in five drafts, four wave frequencies and four wave heights, and their classification is given in Table 5. So, there are 16 distinct tests in each draft. A total of 240 tests were carried out during this part of the experiments.

To determine the accuracy of the results and the subsequent error from the averaging, an error analysis was performed for this step. For this, the standard deviation (σ) of the data was calculated. The standard deviation indicates the difference between the data from the mean value and is obtained from the following equation.

$$\sigma = \sqrt{\frac{\sum_{j=1}^{n}(\overline{X}-X_i)^2}{n-1}} \qquad (12)$$

where X_i is the value of a parameter for each test, $\overline{X}$ the mean value of this parameter and n the number of replicates of the tests (in this experiments; n=3). If the standard deviation is close to zero, this indicates that the data is close to the average and have a little dispersion, while a high standard deviation represents a significant dispersion of data. To estimate the accuracy, a standard error (S) is required. The standard error can be expressed as:

$$S = \frac{\sigma}{\sqrt{n}} \qquad (13)$$

Figure 13 shows the error analysis of the pressure data associated with 16 tests for the 2cm draft. The horizontal axis represents the 16 different tests for four wave heights and four wave periods shown in Table 5. In this figure, raw and mean value of pressure for the three replicates, standard deviation (σ) and standard error (S) are indicated.

According to Figure 13, it can be seen that in most cases, the standard deviation and the standard error are less than 10 Pa and 5 Pa, respectively.

After determining the error for each test, the highest error rate is calculated in all tests for each draft. Based on the results, the maximum error is about 5.8%, which is related to test No. 1. This trend was carried out for the other four drafts, and the highest error in drafts of 6, 10, 14 and 18 cm is 6.7%, 7.4%, 8.5%, and 9.9%, respectively.

4. 2. Results   First, the results are compared for two orifice diameters of 80 and 32 mm. The effect of the diameter of air outlet duct in waves with a constant wave
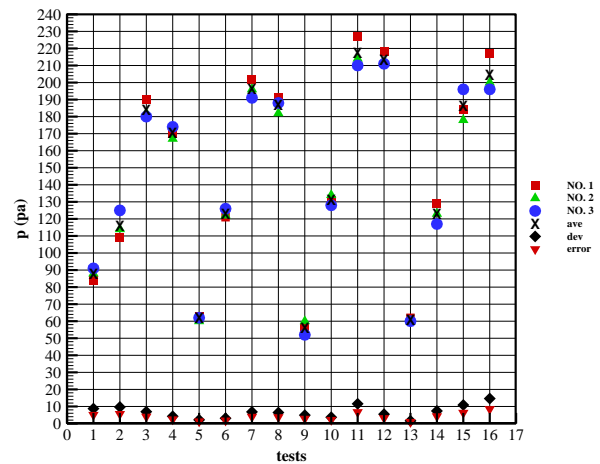

Figure 13. Mean pressures, average of 3 mean pressures and their standard deviation (draft = 2 cm)

height of 5 cm and wave frequencies of 0.67 and 0.83 Hz in the 6 cm draft was investigated. Figure 14 illustrates the average pressure and average airflow rate for each duct diameter.
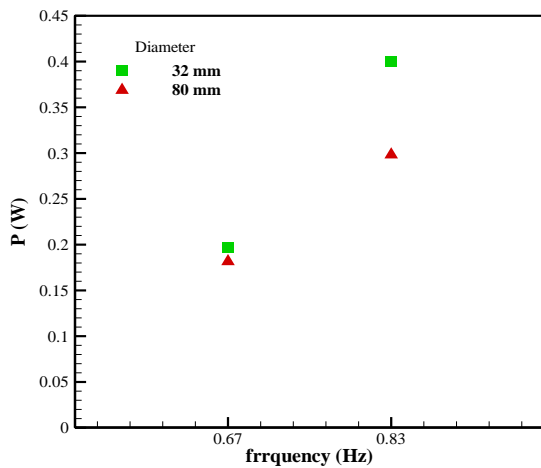
Figure 15 compares the pneumatic power for two duct diameters.

It can be observed that the pressure inside the chamber with 32 mm diameter is higher, but its air outlet flow rate is less than that of the chamber with 80 mm diameter. However, creating a diameter of 32 mm in the air outlet increases the power of the converter, as the multiplication of the pressure and the outlet airflow, which gives the pneumatic power, is higher in this chamber. In Figure 16, variations of pneumatic power with the draft at different wave heights are shown for all of the four wave frequencies.
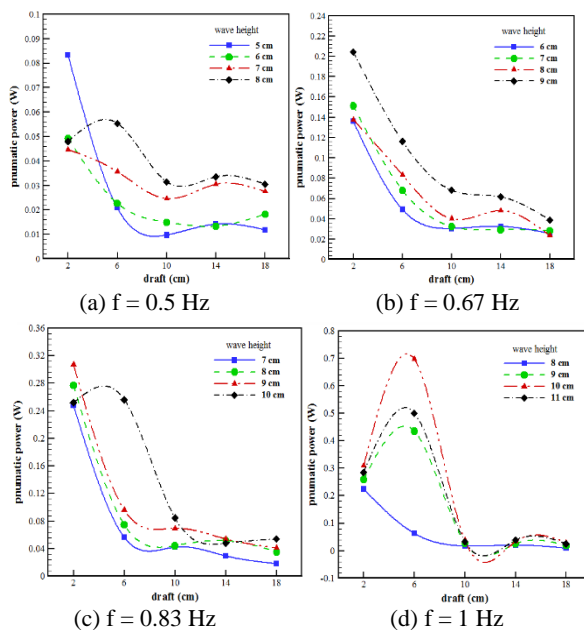
It can be observed that for all wave frequencies, with increasing the wave height, the pneumatic power is increased almost in all points. However, in some cases,
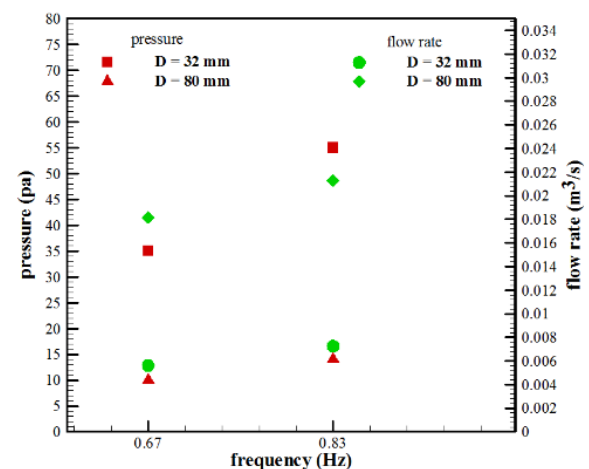
Figure 14. Comparison of pressure and flow rates for two duct diameters

Figure 15. Comparison of pneumatic power for two duct diameters

(a) f = 0.5 Hz

(b) f = 0.67 Hz

(c) f = 0.83 Hz

(d) f = 1 Hz

Figure 16. Variation of pneumatic power with the draft at different wave heights for every four frequencies (0.5, 0.67, 0.83 and 1 Hz)

as in Figure 16 (a), the 5 cm wave height unexpectedly has the highest pneumatic power at the frequency of 0.5 Hz. In addition, as it can be seen in Figure 16 (d), a wave with the height of 10 cm has a greater pneumatic power than the 11 cm wave height. However, the general trend in all of the four wave frequency groups indicates that increasing the wave height leads to an increment in the power of the converter.

In addition, it can be seen that in the frequencies of 0.5, 0.67 and 0.83 Hz, the 2 cm draft has the highest power; the extractable pneumatic power decreases by increasing the draft. This trend also applies for the 8cm wave height and 1 Hz wave frequency but, increasing the

wave height at this frequency causes a sharp increase in the pneumatic power for 6 cm draft; the highest power (0.7 watts) occurs at this frequency and 10 cm wave height.

There are two modes for the collision of waves with the device. The first mode happens when the wave enters the device without encountering the front wall. When the draft is low, the wave enters strongly from the lower gate and compresses the air inside the chamber. The second mode happens when the wave creates a continuous water column in the chamber in such a way that crossing the wave crest and trough from the converter makes the water column to flow up and down. This mode occurs when the draft is increased. In this case, due to the collision of the wave with the front wall, the reflection of incident wave increases and as a result, part of the wave power will be wasted. In addition, as draft rises, the volume of the air column inside the chamber will be reduced, which this also will reduce productive pneumatic power.

When the device's draft is 2 cm, the first mode occurs and with the collision of each wave, the pressure inside the chamber increases. As a result, a relatively high pneumatic power is generated. This mode occurs for a draft of 6 cm at a frequency of 1 Hz. In this case, by increasing the wave frequency and wave height, the waves enter the chamber from the lower gate of the device. In this draft, due to the stronger water column inside the chamber, its productive pneumatic power is increased compared to the 2 cm draft.

The maximum average pneumatic power produced in this model is 0.7 watts. Therefore, considering the scale of 1:22, the pneumatic power of OWC device will be 35 kW. Assuming a 50% power loss in the turbine and generator, the final power of the device will be 17.5 kW.

In the final step, the model capture performance is calculated to determine the conversion rate of the incident wave power to pneumatic power. The capture performance and incident wave power are obtained from Equations (5) and (6), respectively.

To investigate the capture performance, firstly waves with different heights and frequencies are categorized into four groups based on their power. Table 6 shows this categorization.

Figure 17 shows the variation of capture performance with frequency at different drafts for each category of wave power.

Generally, the device has better efficiency in 2 cm draft for all wave powers. However, the maximum efficiency is related to the 6 cm draft at the frequency of 1 Hz (except for waves having the power of 4-5 watts). The results also indicate that the model has very low efficiency in 10, 14 and 18 cm drafts. This means that in constant wave power, the pneumatic power produced by the model has decreased and this is evident in the pneumatic power diagrams (Figure 16).

TABLE 6. Waves categorization based on wave power

power (W)	f (Hz)	H (cm)
4-5	0.5	5
	0.67	6
	0.83	7
	1	8
6-7	0.5	6
	0.67	7
	0.83	8
	1	9
8-9	0.5	7
	0.67	8
	0.83	9
	1	10
10-11	0.5	8
	0.67	9
	0.83	10
	1	11

Figure 17. Capture performance versus frequency at different drafts for four categories of wave power

The efficiency of the 2 cm draft decreases with increasing wave power (at similar frequencies). The efficiency decrement does not necessarily mean reducing pneumatic power. It is important to note that, although the capture performance indicates the conversion rate of the incoming wave power to pneumatic power, the most important parameter for the OWC is the generated pneumatic power because this power makes the turbine to circulate.

At 2 and 6 cm drafts, the efficiency increases with increasing the wave frequency. The factor to be considered here is the ratio of b/λ (where b is the chamber width, and λ is the wavelength). The wavelengths for frequencies of 0.5, 0.67, 0.83 and 1 Hz are 4.5, 2.6, 1.7 and 1.2 meters respectively. Increasing the frequency reduces the wavelength and thus increases the b/λ ratio (b = 0.24 m). This means that the converter has taken a larger share from the wave with less length. Therefore, in constant wave power, a wave with a shorter wavelength has higher capture performance. Sheng et al. analyzed this phenomenon and concluded that long waves might by-pass the small wave energy device easily, hence, its power capture capacity will be very limited [14]. It should be noted that this conclusion only applies to this model with the mentioned wave characteristics. However, in general, it is predicted that if the value of dimensionless number $\frac{b}{\lambda/2}$ is closer to 1 (or b/λ to 0.5), the capture performance will be higher.
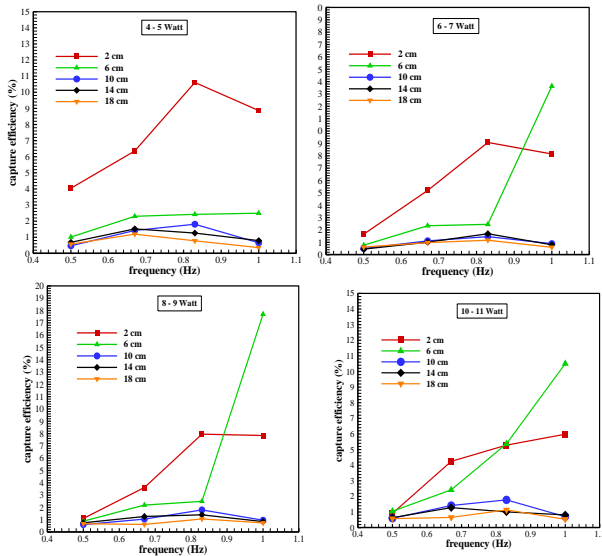
5. CONCLUSION

In this study, the power available in a fixed onshore OWC wave energy converter according to the wave characteristics of the Oman Sea in the Chabahar port was evaluated. For this purpose, the waves were scaled for laboratory conditions firstly. Then, a model of the device was tested on the wave tank, and the effects of wave height and wave frequency, the front wall draft and the diameter of the air outlet channel were investigated. These experiments were repeated three times to ensure the accuracy of the data. The error analysis showed that the scattering of data is low and the results match well.

In the first stage of the experiments, according to the studies conducted in the literature, the effect of duct diameter was compared for two diameters of 80 and 32 mm. The results showed improvement in pneumatic power for the diameter of 32 mm.

In the next step, the effect of wave characteristics (height and frequency) in different drafts was investigated. The results at this stage indicate that generally increasing the wave height increases the pneumatic power of the device and increasing the draft decreases the pneumatic power. However, at the frequency of 1 Hz, the maximum pneumatic power was achieved in a 6 cm draft.

Based on these results, reducing the wavelength will increase the wind power. For more energy extraction from a stronger wave, a larger device is desirable. In general, it is predicted that if the value of the dimensionless number $\frac{b}{\lambda/2}$ is closer to 1 (or b/λ to 0.5), the capture performance will be more.

The maximum average pneumatic power achieved in these tests is 0.7 watts, which corresponds to 35 kW at

full scale (1:22). Assuming 50% loss in turbine and generator, a single OWC system with a capacity of 17.5 kW would be achievable. The capture performance of the model for this test case is 18%, so it can be seen that by optimizing the device geometry and increasing the wave power absorption, the system capacity can be improved.

6. REFERENCES

1. Alamian, R., Shafaghat, R. and Safaei, M.R., "Multi-objective optimization of a pitch point absorber wave energy converter", *Water*, Vol. 11, No. 5, (2019), 969.

2. Amiri, H.A., Shafaghat, R., Alamian, R., Taheri, S.M. and Shadloo, M.S., "Study of horizontal axis tidal turbine performance and investigation on the optimum fixed pitch angle using cfd", *International Journal of Numerical Methods for Heat & Fluid Flow*, Vol. ahead-of-print, (2019). DOI: 10.1108/HFF-05-2019-0447

3. Ebrahimpour, M., Shafaghat, R., Alamian, R. and Safdari Shadloo, M., "Numerical investigation of the savonius vertical axis wind turbine and evaluation of the effect of the overlap parameter in both horizontal and vertical directions on its performance", *Symmetry*, Vol. 11, No. 6, (2019), 821.

4. Alamian, R., Shafaghat, R., Miri, S.J., Yazdanshenas, N. and Shakeri, M., "Evaluation of technologies for harvesting wave energy in caspian sea", *Renewable and Sustainable Energy Reviews*, Vol. 32, No., (2014), 468-476.

5. Alamian, R., Shafaghat, R., Farhadi, M. and Bayani, R., "Experimental evaluation of irwec1, a novel offshore wave energy converter", *International Journal of Engineering-Transactions C: Aspects*, Vol. 29, No. 9, (2016), 1292-1299.

6. Bin, Y.O., Tawi, K. and Suprayogi, S.D., "Computer simulation studies on the effect overlap ratio for savonius type vertical axis marine current turbine", *International Journal of Engineering-Transactions A: Basics*, Vol. 23, No. 1, (2010), 79-88.

7. Yaakob, O., Suprayogi, D., Ghani, M.A. and Tawi, K., "Experimental studies on savonius-type vertical axis turbine for low marine current velocity", *International Journal of Engineering-Transactions A: Basics*, Vol. 26, No. 1, (2012), 91-98.

8. Falcão, A.F. and Henriques, J.C., "Oscillating-water-column wave energy converters and air turbines: A review", *Renewable Energy*, Vol. 85, No., (2016), 1391-1424.

9. Holzhauer, E., "Assessment of the power available in a fixed offshore oscillating water column plant", Cranfield University, School Of Engineering, MSc Thesis, (2012),

10. Suroso, A., "Hydraulic model test of wave energy conversion", *Jurnal Mekanikal*, Vol. 19, (2005), 84-94.

11. Morris-Thomas, M.T., Irvin, R.J. and Thiagarajan, K.P., "An investigation into the hydrodynamic efficiency of an oscillating water column", *Journal of Offshore Mechanics and Arctic Engineering*, Vol. 129, No. 4, (2007), 273-278.

12. Ram, K., Faizal, M., Ahmed, M.R. and Lee, Y.-H., "Experimental studies on the flow characteristics in an oscillating water column device", *Journal of Mechanical Science and Technology*, Vol. 24, No. 10, (2010), 2043-2050.

13. Dizadji, N. and Sajadian, S.E., "Modeling and optimization of the chamber of owc system", *Energy*, Vol. 36, No. 5, (2011), 2360-2366.

14. Sheng, W., Lewis, A. and Alcorn, R., "On wave energy extraction of oscillating water column device", in 4th International Conference on Ocean Energy, Dublin, Ireland. (2012).

15. Viviano, A., Naty, S., Foti, E., Bruce, T., Allsop, W. and Vicinanza, D., "Large-scale experiments on the behaviour of a generalised oscillating water column under random waves", *Renewable Energy*, Vol. 99, (2016), 875-887.

16. Ning, D.-Z., Wang, R.-Q., Zou, Q.-P. and Teng, B., "An experimental investigation of hydrodynamics of a fixed owc wave energy converter", *Applied Energy*, Vol. 168, (2016), 636-648.

17. Alamian, R., Shafaghat, R., Hosseini, S.S. and Zainali, A., "Wave energy potential along the southern coast of the caspian sea", *International Journal of Marine Energy*, Vol. 19, (2017), 221-234.

18. Zabihian, F. and Fung, A.S., "Review of marine renewable energies: Case study of iran", *Renewable and Sustainable Energy Reviews*, Vol. 15, No. 5, (2011), 2461-2474.

19. Zanous, S.P., Shafaghat, R., Alamian, R., Shadloo, M.S. and Khosravi, M., "Feasibility study of wave energy harvesting along the southern coast and islands of iran", *Renewable Energy*, Vol. 135, (2019), 502-514.

20. "Modeling of iranian sea waves, volume ii: Persian gulf and oman sea", 1st ed, Ports and Maritime Organization, (2008).

21. Alamian, R., Shafaghat, R., Shadloo, M.S., Bayani, R. and Amouei, A.H., "An empirical evaluation of the sea depth effects for various wave characteristics on the performance of a point absorber wave energy converter", *Ocean Engineering*, Vol. 137, (2017), 13-21.

22. Fairhurst, J., "Modelling and design of an oscillating wave energy converter", Stellenbosch University, Faculty of Engineering, MSc Thesis, (2015),

23. Day, S., Penesis, I., Babarit, A., Fontaine, A., He, Y., Kraskowski, M., Murai, M., Salvatore, F. and Shin, H., "Ittc recommended guidelines: Wave energy converter model test experiments (7.5-02-07-03.7)", in 27th International Towing Tank Conference. (2014), 1-13.

24. Alamian, R., Shafaghat, R., Bayani, R. and Amouei, A.H., "An experimental evaluation of the effects of sea depth, wave energy converter's draft and position of centre of gravity on the performance of a point absorber wave energy converter", *Journal of Marine Engineering & Technology*, Vol. 16, No. 2, (2017), 70-83.

25. Kooverji, B., "Pneumatic power measurement of an oscillating water column converter", Stellenbosch: Stellenbosch University, (2014),

26. Joubert, J.R., "Design and development of a novel wave energy converter", Stellenbosch University, Faculty of Engineering, Doctor of Engineering Thesis, (2013),

27. Thiruvenkatasamy, K. and Neelamani, S., "On the efficiency of wave energy caissons in array", *Applied Ocean Research*, Vol. 19, No. 1, (1997), 61-72.

Experimental Assessment of a Fixed On-Shore Oscillating Water Column Device: Case Study on Oman Sea

H. Yazdi, R. Shafaghat, R. Alamian

Sea-Based Energy Research Group, Babol Noshirvani University of Technology, Babol, Iran

چکیده

اقیانوس یکی از منابع تجدیدپذیر انرژی است که تاکنون روش‌های گوناگونی برای استحصال انرژی از آن به‌کار رفته است. ستون نوسانی آب قابل نصب در ساحل، یکی از سامانه‌های جذب انرژی از امواج دریاست که به دلیل ساختار ساده‌اش مورد توجه قرار گرفته است. بررسی توان بادی در این سامانه به‌دلیل این که تبدیل انرژی موج به انرژی بادی، اولین فرایند تبدیل انرژی می‌باشد، بسیار حائز اهمیت است. هدف این مطالعه، ارزیابی توان قابل دسترس در یک دستگاه ستون نوسانی آب ثابت ساحلی با توجه به مشخصات امواج دریای عمان در سواحل بندر چابهار می‌باشد. بدین منظور مدلی از این مبدل انرژی به‌صورت تجربی در استخر موج آزمایش شده و توان بادی تولیدی آن مورد ارزیابی قرار گرفت. در این آزمایش‌ها، تاثیر پارامترهای ارتفاع و بسامد موج، فاصله سطح آب از لبه دیواره جلویی دستگاه (آبخور) و قطر کانال خروجی هوا بررسی شده است. نتایج نشان می‌دهند که افزایش ارتفاع موج به‌طور کلی باعث افزایش توان بادی می‌شود و نیز تغییرات این توان با آبخور مدل، به فرکانس امواج برخوردی بستگی دارد. راندمان جذب مدل در بهترین حالت ۱۸٪ است که توان بادی حداکثر نیز در این حالت تولید می‌شود و برابر با ۰/۷ وات می باشد

doi: 10.5829/ije.2020.33.03c.14